ELSEVIER

Journal of Crystal Growth 173 (1997) 277–284

JOURNAL OF CRYSTAL GROWTH

Structural characterization and surface lattice strain determination of ZnS/GaAs heterostructures grown by metalorganic vapour phase epitaxy

G. Leo[a,*], L. Lazzarini[b], N. Lovergine[c], F. Romanato[d], A.V. Drigo[d]

[a] *Istituto per lo studio di nuovi Materiali per l'Elettronica (IME), CNR, Via per Arnesano, I-73100 Lecce, Italy*
[b] *MASPEC, CNR, Via Chiavari 18 A, I-43100 Parma, Italy*
[c] *Dipartimento di Scienza dei Materiali and Istituto Nazionale per la Fisica della Materia, Via per Arnesano, I-73100 Lecce, Italy*
[d] *Dipartimento di Fisica "G. Galilei" and Istituto Nazionale per la Fisica della Materia, Via Marzolo 8, Padova, Italy*

Received 8 October 1996; accepted 2 November 1996

Abstract

We report on the structural characterization of ZnS epilayers grown on (1 0 0)GaAs by metalorganic vapour-phase epitaxy (MOVPE). The crystalline quality at the ZnS epilayer surface and the defect depth distribution was studied by Rutherford Backscattering Spectrometry (RBS)-ion channeling measurements as a function of the epilayer thickness. Transmission electron microscopy (TEM) observations were performed on selected ZnS/GaAs heterostructures. Misfit dislocations (MD) were observed at the ZnS/GaAs interface. In addition, a high density of planar defects such as stacking faults (SF) and microtwins (MT) were identified into the epilayer up to 200–300 nm. The density of these defects decreases by increasing the epilayer thickness, but a quite high and constant density of microtwins still occurs in epilayers thicker than 400 nm. However, absorption measurements point out a high optical quality for all the measured ZnS epitaxial layers. Finally, surface lattice strain was determined in the ZnS/GaAs samples by ion channeling measurements. Our data indicate that the initial lattice misfit is already fully relaxed in epilayers as thick as 400 nm and only a small residual thermal strain is measured in thicker samples.

1. Introduction

ZnS is a wide band-gap II–VI semiconductor ($E_g = 3.75$ eV) of relevant technological interest for the realization of ZnSe/ZnS, ZnSSe/ZnS and ZnCdSe/ZnS strained layer superlattices and multiple quantum well heterostructures to be used for UV and blue light emitting optoelectronic devices [1, 2]. In this respect the lack of high-quality, low-cost ZnS single-crystal wafers makes it necessary to grow high crystalline quality epitaxial ZnS buffer layers on suitable alternative substrates such as GaAs.

Several attempts have been previously reported in the literature to achieve high crystalline and optical quality ZnS epilayers by both metalorganic vapour-phase epitaxy (MOVPE) [3–5] and

* Corresponding author.

PII S0022-0248(96)00972-4

molecular beam epitaxy (MBE) [6–8]. In spite of the quite high optical quality shown by these epilayers, the crystalline quality is not optimized yet. Recently, a first report on the optimization of the structural and optical properties of ZnS epilayers grown by MOVPE on (1 0 0) GaAs by studying epilayers grown under different VI/II precursor molar flow ratios (MFR) and as a function of the in-situ substrate annealing temperature has been published by some of the present authors [9]. However, the occurrence of both high lattice and thermal mismatches between ZnS and GaAs strongly affects the structural quality of the ZnS epilayers. In fact, a fairly high density of misfit dislocations (MD) is expected to be generated close to the ZnS/GaAs interface. Moreover, recent TEM observations of the ZnS/GaAs heterostructure [10] have also evidenced a high density of microtwins starting at the GaAs interface. The propagation of these microtwins seems to be mainly growth dominated whereas their nucleation remains still ambiguous and either a growth or a stress-related mechanism would be viable as reported in Ref. [10].

In this paper, a detailed structural characterization of MOVPE grown ZnS epilayers as a function of their thickness by means of ion channeling Rutherford Backscattering Spectrometry (RBS) and TEM observations is reported. Also the amount of residual lattice strain was accurately determined by ion channeling measurements and compared with the expected thermal strain.

2. Experimental procedure

ZnS epilayers were grown on (1 0 0)GaAs in an Aixtron 200RD MOVPE reactor by using (t-Bu)SH and Me_2Zn:Et_3N as S and Zn precursors, respectively. Semi-insulating LEC-grown (1 0 0) $\pm$ 0.25° GaAs was used as substrate. For all growth runs the temperature of the annealing process was 550°C and the transport rate of Me_2Zn:Et_3N was set to achieve precursors MFRs ($F_{(t\text{-}Bu)SH}/F_{Me2Zn:Et3N}$) around 5.16. The growth was performed at 304 mbar chamber pressure and 342°C. More details of substrate preparation and growth conditions were reported elsewhere [9, 11]. The ZnS epilayers studied in the present work had thickness ranging from 170 to 900 nm.

The structural characterization of the ZnS epilayers was performed by Rutherford Backscattering Spectrometry (RBS) measurements at the Laboratori Nazionali di Legnaro (Italy). To this purpose, $^4He^+$ beams of 2 and 3.5 MeV energy were used as primary ion beams following the epilayer thicknesses. A goniometer sample holder with both repeatability and overall precision of 0.01° was used for the ion channeling measurements. Surface strain measurements were performed by recording the angular yield curves from a surface region for several lattice directions inclined to the surface normal [12].

Bright field, dark field and high-resolution transmission electron microscopy (TEM) observations were performed by using a JEOL 2000 FX microscope on ⟨1 1 0⟩ oriented cross-sections and (0 0 1) plan view. The sample cross sections were prepared by mechanochemical thinning followed by Ar^+ and I^+ ion-milling on a Gatan 600 DUO-MILL system.

A quantitative evaluation of the ZnS epilayer surface roughness was obtained for all samples by using a Tencor Instrument Model 200 Alpha-step surface profiler, having a vertical resolution of 0.5 nm. Several 40 μm surface scans at a sampling rate of 25 point/μm were performed for each epilayer. This allowed us to calculate the value of the ZnS surface average roughness R_a, i.e. the arithmetic average of the surface height deviations from the mean surface height along the scan line [13].

3. Results

Typical ZnS/GaAs RBS spectra in both random and [1 0 0] aligned conditions are reported in Fig. 1 together with the computer simulation of the random spectrum. Computer simulations of the random spectra allow us to estimate the epilayer thickness with a systematic error lower than 10%, depending on the uncertainities in the Zn and S stopping powers [14]. The computer simulation takes into account both the experimental energy resolution (detector and associated electronic) and beam energy straggling in the way in and out in the sample. In order to obtain a good agreement

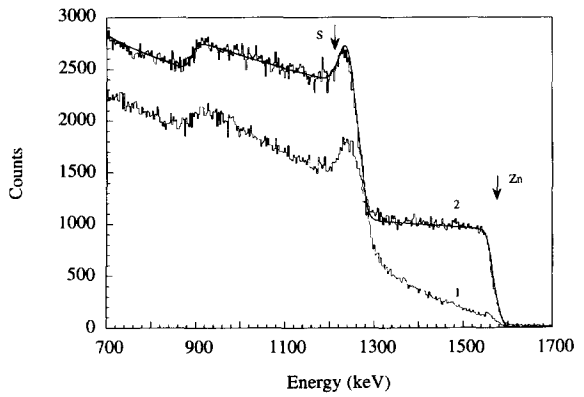

Fig. 1. 2.0 MeV $^4He^+$ RBS spectra of a ZnS/GaAs heterostructure: (1) [1 0 0] aligned; (2) random geometry. The ZnS thickness is 586 nm. The computer simulation of the random spectrum is also reported for comparison (solid line). The arrows indicate scattering energies from the elements at the surface.

between the simulated and the experimental spectra, it was necessary to introduce a linearly graded composition profile at the ZnS/GaAs interface. The thickness, Δt, of this composition tail is reported in Table 1 for different ZnS epilayer thickness. For ZnS thicknesses below 0.6 μm Δt appears to be thickness independent with an average value of (36 ± 4) nm. It must be underlined that the RBS technique does not discriminate between elemental interdiffusion at the heterointerface and interface or surface roughness-induced effects. Hence, additional surface profiling measurements of the ZnS average surface roughness, R_a, have been performed in order to clarify this point. The R_a values are also reported in Table 1. If only surface roughness is present it causes a film thickness distribution which is assumed to be Gaussian with standard deviation $\sigma = \sqrt{\pi/2}R_a \cong 1.25R_a$. The interface region of the RBS ZnS concentration profile would thus result in an error function (erf). Within the sensitivity of the RBS technique the erf is approximated by a linearly graded concentration profile whose width Δt corresponds to nearly 4σ. By looking at the data in Table 1 it appears that experimental Δt values are significantly higher than $5R_a$ so that interface broadening must also be assumed. The interface broadening can be the result of interface roughness and/or of elemental interdiffusion.

Table 1
Average surface roughness, R_a, and RBS composition tail, Δt, as a function of the ZnS thickness, t_{ZnS}; the calculated interface broadening, σ_D, is also reported

t_{ZnS} (nm)	Δt (nm)	R_a (nm)	σ_D (nm)
176	40 ± 4	2.0 ± 0.8	9.7 ± 1.1
204	36 ± 4	1.4 ± 0.5	8.8 ± 1.0
261	32 ± 8	1.6 ± 0.5	7.7 ± 2.1
308	40 ± 4	1.5 ± 0.5	9.8 ± 1.0
415	39 ± 4	2.7 ± 0.8	9.1 ± 1.1
485	36 ± 4	2.6 ± 0.8	8.4 ± 1.1
586	30 ± 4	3.5 ± 0.7	6.1 ± 1.4
897	47 ± 4	5.5 ± 1.0	9.5 ± 1.5

Both these processes would result in an erf-like interface RBS composition profile characterized by the standard deviation σ_d, that can be calculated from the total width Δt by deconvolution of the surface roughness. The σ_d values are also reported in Table 1. Within the accuracy of this analysis it appears that, for all sample thicknesses, σ_d is constant at a value of (8.6 ± 1.2) nm. This fact points to a significant interface broadening of about 30 nm that must occur in the early stages of the growth. Atomic force microscopy (AFM) observations, performed on selected ZnS/GaAs samples, have shown that the stylus profilometer underestimates the R_a value. Anyway, as the AFM roughness values are still very low as compared to Δt, the use of these values does not produce any significant variation in the results of our analysis.

The ion channeling spectrum shows a fairly high dechanneling rate by increasing the beam penetration depth, indicating the existence of a high density of extended defects mainly close to the ZnS/GaAs interface. In order to obtain informations about the depth distribution of the defects occurring in the ZnS epilayer, the dechanneling probability, $P_D(z)$, has been calculated following the relationship: $P_D(z) = \ln(1 - \chi_V(z))/(1 - \chi_D(z))$ [15], where z is the depth below the ZnS surface, χ_D is the epilayer channeling yield normalized to the random yield and χ_V is the corresponding yield for a perfect crystal. As the surface minimum yields, χ_{min}, previously measured for VPE grown ZnS epilayers thicker than 1 μm compare well with the semi-empirical value expected for an ideal ZnS

crystal [16], in our calculations we assumed $\chi_V(z)$ to coincide with the normalized yield of a 4 μm thick VPE grown epilayer [17].

In Fig. 2 the dechanneling probability, calculated for three samples 308, 586, and 897 nm thick, is shown as a function of the distance from the surface. For all samples a sharp increase in the dechanneling probability is observed in a region of about 200–300 nm from the ZnS/GaAs interface. As the derivative of the dechanneling probability, $dP_D(z)/dz$, is proportional to the local defect concentration, $n_D(z)$, this result shows that the highest defect density is present in a near interface region. Moreover, in the near surface region the dechanneling probability, P_D, of the thickest samples increases linearly with z indicating a constant density of defects.

The crystalline quality at the epilayer surface can be estimated by the value of the channeling yield at the sample surface (χ_{min}). χ_{min} values as a function of the ZnS thickness are reported in Fig. 3. The sharp decrease of χ_{min} from 36% down to 12% by increasing the epilayer thickness from 200 to 500 nm points out a strong improvement in the epilayer crystalline quality at the surface as already suggested by the dechanneling analysis. However, no further surface quality improvement was found for epilayer thicker than 500 nm and the χ_{min} value saturates around 12%. This value is much higher than both the theoretical value for a perfect ZnS

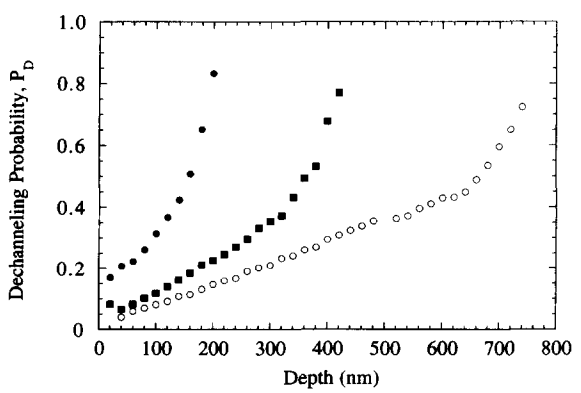

Fig. 2. Dechanneling probability, P_d, as a function of the depth below the ZnS surface for epilayers having different thickness: 897 nm (○); 586 nm (■) and 308 nm (●).

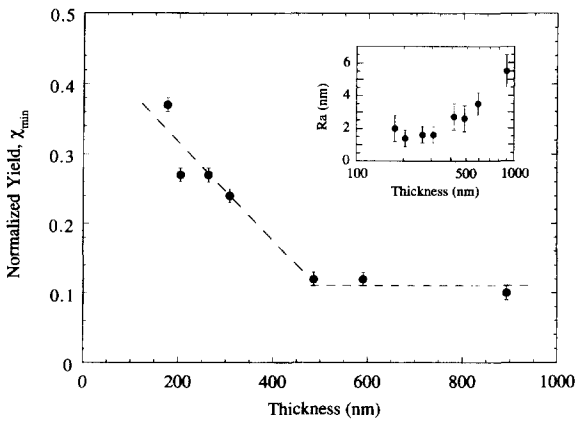

Fig. 3. Values of the [1 0 0]-channeling surface yield normalized to the random yield, χ_{min}, as a function of the ZnS thickness. The average surface roughness values, R_a, are reported in the inset as a function of the epilayer thickness.

crystal and the experimental value previously found for ZnS epilayers grown by vapour-phase epitaxy (VPE) [17]. This indicates that, although the surface crystalline quality of the ZnS epilayers is definitely strongly improved, a remarkable density of extended defects still exists even at the surface of samples as thick as about 1 μm in agreement with the previous analysis.

The surface roughness values, R_a, are reported as a function of the epilayer thickness in the inset of Fig. 3. The surface morphology appears to be quite smooth (< 2 nm) and uniform for thicknesses below 400 nm. Above this thickness it raises to 5.5 nm at 0.9 μm. This behaviour shows that the surface morphology is independent of the surface crystalline quality. On the other hand, a similar behaviour has been reported in Ref. [18] and a clear explanation is still lacking.

TEM observations have been performed on selected samples in order to investigate the defect distribution and nature. Fig. 4 shows a (1 1 0) cross-section micrograph of a 586 nm thick ZnS epilayer taken in dark field two-beam strong condition with a (2 2 0) type reflection. The mottled appearence of the layer is a residual of the ion-beam thinning that in our laboratory is not a well assessed procedure for the II–VI compounds. Following Cullis' work [19] our results are randomly

Fig. 4. Dark field TEM micrograph ($g = 220$) of a 620 nm thick ZnS/GaAs sample cross section. The planar defect density decreases approaching the surface.

Fig. 5. (1 1 0) zone axis high-resolution image of the typical defect arrangement in the epilayer close to the interface showing that most of the planar defects annihilate each other.

successful. Anyway, in this case, this artifact does not affect the extended defect analysis.

The density of extended defects is very high within 200 nm of the heterointerface and decreases approaching the surface as expected from the RBS results. Planar defects lying along {1 1 1} planes and exhibiting fringe contrast propagate through the entire epilayer. After Chen and Stobbs [20] some of these defects have been identified as microtwins (MTs) rather than stacking faults (SFs) (MTs and SFs are so closely structurally related that intrinsic and extrinsic SFs may be thought as one-layer and two-layer MTs, respectively). The number of such microtwins appears to be independent of the epilayer thickness in good agreement with the RBS-channeling results. Plan view investigations of the same sample evidence comparable planar defects density for the two orthogonal ⟨1 1 0⟩ directions, which is not a common result [10]. The surface roughness investigated along several microns can locally be much larger than R_a: in this micrograph a surface height difference of about 30 nm can be measured.

The interface region has been investigated in the high-resolution mode after further I^+ ion milling of the sample. Fig. 5 reports a typical stacking disorder arrangement: almost all the planar defects originating at the interface and annihilating within about 100 nm of the interface are intrinsic and extrinsic SFs. 60° and 90°-type misfit dislocations (MD) are also present at the heterointerface. Obviously, partial dislocations terminating SFs and MTs are observed into the ZnS epilayer.

Both in conventional and high-resolution observations, the ZnS/GaAs interface appears quite smooth. In this respect, the broadening assumed to fit the RBS experimental spectra must be totally ascribed to the surface roughness and to the compositional tail which could be not revealed by TEM analysis.

Despite the high defect density revealed by both RBS-channeling and TEM measurements, the present ZnS epilayers show a high optical quality. In fact, the analysis of the 10 K absorption spectrum previously published by some of the present authors [9] shows that a sharp excitonic peak arises from both light-hole (LH) and heavy-hole (HH) excitonic resonance contributions. The full-width at half-maximum (FWHM) of the LH and HH resonance is equal to 5.2 ± 0.3 and 5.6 ± 0.2 meV, respectively, demonstrating the high optical quality of the present samples that is even better than some of the recent results reported in the literature [21]. Details on optical spectroscopy measurements of the present samples will be reported elsewhere [22].

In order to study the strain relaxation mechanism in the ZnS/GaAs heterostructure, strain

measurements have been also performed by ion channeling as a function of the ZnS thickness. These measurements allow us to deduce the value of the tetragonal distortion, $\varepsilon_T = a_\perp/a_\parallel - 1$, where $a_\perp$ and $a_\parallel$ are the ZnS lattice parameter perpendicular and parallel to the ZnS/GaAs interface, respectively. The strain parallel to the interface, $\varepsilon_\parallel$, has been then calculated from the relationship: $\varepsilon_\parallel = -\varepsilon_T/(1+\alpha)$ where $\alpha = 2C_{12}/C_{11} = 1.28$ for ZnS [23]. Fig. 6 shows the values of $\varepsilon_\parallel$ at the epilayer surface as a function of the ZnS thickness. It appears that $\varepsilon_\parallel$ rapidly decreases by increasing the epilayer thickness. The high initial tensile lattice misfit between ZnS and GaAs, $f = 4.5\%$, is almost totally relaxed for a ZnS thickness of 200 nm. A further slight relaxation takes place by increasing the ZnS thickness up to 400 nm where $\varepsilon_\parallel = (0.07 \pm 0.01)\%$. For ZnS epilayers thicker than 400 nm a small and constant tensile residual strain was measured by both ion channeling and absorption measurements [22], its average value being: $\varepsilon_\parallel = (0.08 \pm 0.02)\%$. This value compares well with the expected thermal strain contribution to the total in-plane surface strain induced in the ZnS/GaAs heterostructure during the cooling down from the growth temperature (342°C) to the RBS measurement temperature (20°C). In fact, by using the currently available ZnS and GaAs linear expansion coefficient data [24, 25] such thermal strain value has been calculated to be $\varepsilon_{\Delta T} = 0.075\%$.

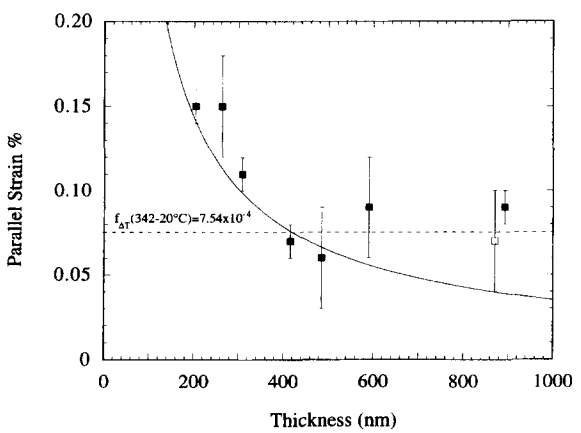

Fig. 6. Parallel strain values as a function of the ZnS thickness. (■) RBS-channeling measurements; (□) absorption measurements. The calculated thermal misfit between the growth temperature (342°C) and the room temperature (20°C) is reported as a dashed line. The solid line represents the prediction of the equilibrium model [29].

4. Discussion and conclusions

ZnS epilayers grown by MOVPE on (1 0 0) GaAs exhibit a fair structural quality that cannot be improved by growing thicker. Both dechanneling analysis and TEM observations have shown that a high density of extended defects exists in a region almost 200–300 nm thick close to the ZnS/GaAs interface. MTs and SFs are present in this region with a decreasing density by increasing the distance from the heterointerface. Contrary to other II–VI/III–V heterostructures [26], in the present samples we did not observe TDs in cross section. Anyway, as the very complicated defect arrangement made it not possible to perform standard defect analysis, TDs not in excess of 10^6 cm^{-2} can be present in this sample. In ZnS epilayers thicker than 400 nm only a residual density of microtwins, lying along the {1 1 1} planes, is clearly evident in the surface region in TEM micrographs. These microtwins start at the ZnS/GaAs interface and extend through the whole epilayer with a constant density.

The ZnS/GaAs interface appears to be flat. In order to explain the RBS composition tail the occurrence of an interfacial interdiffusion of about 30 nm has to be taken into account. As a striking feature this noticeable diffusion lenght appears to be independent of the epilayer thickness, i.e. of the growth time. A defect enhanced diffusion mechanism or/and an auto-doping process due to 3D growth in the first growth stage could play an important role in this time-independent elemental interdiffusion at the ZnS/GaAS interface. However, at present, we are not able to give a clear explanation of such anomalous diffusion process.

In spite of the fair crystalline quality of the present samples, their optical quality appears to be excellent. A detailed discussion of the contradiction between the structural quality of the present ZnS epilayers as derived from RBS and optical measurements will be reported elsewhere [27].

The initial tensile lattice misfit existing between ZnS and GaAs is totally relaxed at the growth temperature for epilayer thicknesses around 400 nm. Unlike the case of strain relaxation in III–V heterostrucutres having tensile misfit [28], no cracks were ever observed in our samples. The strain relaxation process appears to proceed in agreement with the equilibrium model [29]. Neverthless, at room temperature the samples are still under a small tensile strain because of the thermal misfit.

As for the strain relaxation process is concerned, our investigation cannot discriminate between the contribution of MDs at the heterointerface and/or of partial dislocations into the epilayer. Anyway, even if our observations do not allow us to precisely determine the MD density and their distance distribution, it is evident that their density is not enough to fully relax the initial lattice misfit. Hence, a relevant contribution due to the partial dislocations associated with the SFs both at the interface and into the epilayer must be taken into account in the relaxation process. As a consequence a strain gradient in the first 400 nm of the ZnS epilayer should be present, as already observed in the ZnTe/GaAs system [26].

The occurrence of such high density of microtwins in the ZnS buffer layer which thread also through the overgrown MQW [30] is a strong limit to the use of these systems for technological applications. In fact, it is well known that microtwins, as well as every stacking disorder, act as sites for small dislocation loop formation when intersecting the active region of II–VI devices [31]. These dislocations are referred to as degradation defects. In fact they behave as non-radiative recombination centers and are responsible for the rapid device degradation. In order to use the ZnS/GaAs heterostructure as substrates for growing ZnS based MQW operating as deep-blue emitting devices, it is thus mainly necessary to eliminate the microtwins or to strongly reduce their density. Microtwins can be nucleated either as a result of heterogeneities in the initiation of the growth or to relieve misfit stress. In the present case the former mechanism could be associated to the observed elemental interdiffusion existing at the ZnS/GaAs interface. A detailed investigation of the microtwins has been undertaken in order to understand their nucleation mechanism and to find a way for their elimination. To this purpose other routes can also be followed. Growing on misoriented (0 0 1) substrates or (1 1 1) surfaces could eliminate the twin nucleation or their propagation to the surface. On the other hand, if twin nucleation is stress-driven, growing on substrates with a strongly reduced misfit, such as GaP, should overcome the problem.

Acknowledgements

The authors are deeply indebted to Dr. P. Prete, Mr. M. Fernandez and Prof. R. Cingolani for absorption measurements. Thanks are also due to G. Imbriani and A. Pinna for their help during MOVPE growth and to A. Sambo for his useful technical assistance during RBS measurements.

References

[1] T. Yokogawa, Physica B 191 (1993) 102.
[2] Y. Yamada, Y. Masumoto, J.T. Mullins and T. Taguchi, Appl. Phys. Lett. 61 (1992) 2190.
[3] P.J. Wright, B. Cockayne, P.J. Parbook, A.C. Jones, P. O'Brien and J.R. Walsh, J. Crystal Growth 104 (1990) 601.
[4] K. Nishimura, K. Sakai, Y. Nagao and T. Esaki, J. Crystal Growth 117 (1992) 119.
[5] O. Briot, N. Briot, A. Abounadi, B. Gil, T. Cloitre and R.L. Aulombard, Semicond. Sci. Technol. 9 (1994) 207.
[6] D.F. Foster, I.L.J. Patterson, L.D. James, D.J. Cole-Hamilton, D.N. Armitage, H.M. Yates, A.C. Wright and J.O. Williams, Adv. Mater. Opt. Electron. 3 (1994) 163.
[7] M. Lang, D. Schikara, C. Gliftge, T. Widmer, A. Forstner, G. Brunthaler, M. von Ortenberg and K. Lischka, Semicond. Sci. Technol. 9 (1994) 229.
[8] K.B. Ozanyan, L. May, J.E. Nicholls, J.H.C. Hogg, W.E. Hagston, B. Lunn and D.E. Ashenford, J. Crystal Growth 159 (1996) 89.
[9] G. Leo, N. Lovergine, P. Prete, M. Longo, R. Cingolani, A.M. Mancini, F. Romanato and A.V. Drigo, J. Crystal Growth 159 (1996) 144.
[10] P.D. Brown, Y.Y. Loginov, W.M. Stobbs and C.J. Humphreys, Phil. Mag. A 72 (1995) 39.
[11] N. Lovergine, M. Longo, C. Gerardi, D. Manno, A.M. Mancini and L. Vasanelli, J. Crystal Growth 156 (1995) 45.
[12] A. Carnera and A.V. Drigo, Nucl. Instrum. Methods B 44 (1990) 357.
[13] ANSI Specifications No. B46, I-1978.
[14] J. Ziegler, Stopping and Ranges of Ions in Matter 4, (Pergamon, New York, 1977).

[15] L.C. Feldman, J.W. Mayer and S.T. Picraux, Materials Analysis by Ion Channeling (Academic Press, New York, 1982).
[16] D.S. Gemmel and R.C. Mikkelson, Phys. Rev. B 6 (1972) 55.
[17] N. Lovergine, G. Leo, A.M. Mancini, F. Romanato, A.V. Drigo, C. Giannini and L. Tapfer, Mater. Sci. Eng. B 28 (1994) 55.
[18] G. Leo, M. Longo, N. Lovergine, A.M. Mancini, L. Vasanelli, A.V. Drigo, F. Romanato, T. Peluso and L. Tapfer, J. Vac. Sci. Technol. B 14 (1996) 1739.
[19] A.G. Cullis and N.G. Chew, MRS Proc. 115 (1988) 3.
[20] C.Y. Chen and W.M. Stobbs, Ultramicroscopy 58 (1995) 289.
[21] A. Abounadi, M. Di Blasio, D. Bouchara, J. Calas, M. Averous, O. Briot, N. Briot, T. Cloitre, R.L. Aulombard and B. Gil, Phys. Rev. B 50 (1994) 11677.
[22] M. Fernandez, P. Prete, N. Lovergine, A.M. Mancini, R. Cingolani, L. Vasanelli and M.R. Perrone, to be published.
[23] H. Hartmann, R. Mach and B. Selle, in: Current Topics in Materials Science, Vol. 9, Ed. E. Kaldis (North-Holland, Amsterdam, 1982) p. 36.
[24] C. Giannini, L. Tapfer, T. Peluso, N. Lovergine and L. Vasanelli, J. Appl. Phys. 28 (1995) A125.
[25] O. Madelung, M. Shulz and H. Weiss, Eds., Landolt-Bornstein, Numerical Data and Functional Relationships in Science and Technology, New Series, Group III, Vol. 17a (Springer, Berlin, 1982).
[26] N. Lovergine, F. Liaci, J.-D. Ganiere, G. Leo, A.V. Drigo, F. Romanato, A.M. Mancini and L. Vasanelli, J. Appl. Phys. 78 (1995) 229.
[27] R. Cingolani et al., to be published.
[28] R.T. Murray, C.J. Kiely, M. Hopkinson and P.J. Goodhew, Inst. Phys. Conf. Ser. No. 146 (1995) 207.
[29] J.W. Matthews, in: Epitaxial Growth, Part B (Academic Press, New York, 1975).
[30] M. Mazzer, L. Calcagnile, G. Leo, N. Lovergine, P. Prete, G. Imbriani, R. Cingolani, A.M. Mancini and C. Zanotti-Fregonara, E-MRS 96, Spring Meeting, Strasbourg, France, 4–7 June 1996.
[31] S. Guha, J.M. De Puydt, M.A. Haase, J. Qju and H. Cheng, Appl. Phys. Lett. 63 (1993) 3107.